

WEBSITE: https://fugus-ijsgs.com.ng

ISSNp: 2488-9229; ISSNe: 3027-1118

INTERNATIONAL JOURNAL OF SCIENCE FOR GLOBAL USTAINABILITY

(A PUBLICATION OF FACULTY OF SCIENCE, FEDERAL UNIVERSITY GUSAU, NIGERIA)

Modeling the Dynamics of Monkey pox Virus in the Presence of Carcass and Environmental Transmission

¹Abdulganiy, G. A., ²Adamu, A. B., ²Salaudeen, Y., ³Mamza, J. J.

¹Department of Statistics, Faculty of Physical Science, Modibbo Adama University, Yola Adamawa State, Nigeria. ²Department of Mathematics, Faculty of Physical Sciences, Modibbo Adama University, Yola Adamawa State, Nigeria. ³Department of Mathematics and Statistics, Federal Polytechnic Nyak, Shendam Plateau State.

Corresponding Author's Email & Phone No.: salaudeeyusuf201@gmail.com, +2348038719847 Received on: August, 2025 Revised and Accepted on: September, 2025 Published on: October, 2025

Monkey pox (MPX) is a re-emerging zoonotic disease caused by the monkey pox virus (MPXV), an Orthopoxvirus within the Poxviridae family. In this study, a mathematical model for the dynamics of the monkey pox virus incorporating carcass and environmental transmission within a shared habitat of humans and rodents was presented. The human population is stratified into seven compartments, while the rodent population is divided into four compartments, alongside a compartment representing environmental contamination. Analytical investigations establish the positivity and boundedness of the model solutions and demonstrate the existence of a biologically feasible invariant region. The model admits both disease-free and endemic equilibria, and the basic reproduction number R_0 is derived using the Next Generation Matrix approach. Local and global stability analyses reveal that the disease-free equilibrium is both locally and globally asymptotically stable when $R_0 < 1$. Sensitivity analysis identifies critical parameters influencing disease persistence. Parameters with positive sensitivity indices contribute to increasing R_0 , while those with negative indices contribute to disease control. Numerical simulations support the analytical findings and demonstrate the effects of varying key parameters on the trajectory of human, animal, and environmental compartments. Results show that increasing human vaccination, adequate quarantine of the infected human, promoting behavioral change, and enhancing environmental sanitation significantly reduce the spread of monkey pox in the society. The dynamics of infected and recovered populations under varying rates of transmission, progression, and environmental decay are examined, providing insight into effective intervention strategies. Based on these findings, we recommend control strategies including public awareness campaigns, education on transmission routes, and preventive measures to curb local outbreaks of the monkey pox virus.

1.0 INTRODUCTION

Monkey pox (MPX) is a re-emerging zoonotic disease caused by the monkey pox virus (MPXV), an Orthopoxvirus within the Poxviridae family. Clinically resembling smallpox, MPX is primarily endemic to Central and West Africa, with increasing outbreaks globally (Kanna et al., 2022). The first human case was identified in the Democratic Republic of the Congo in 1970, followed by Nigeria's index case in 1971 (Alakunle et al., 2020). Since then, Nigeria has recorded over 200 confirmed and more than 500 suspected cases (Awoyomi et al., 2023). Globally, 25,391 confirmed cases were reported by August 2022, including significant outbreaks in non-endemic regions (Chadha et al., 2022). MPXV transmission occurs through zoonotic (animal-to-human), human-to-human, and environmental routes. Animal contact—especially with rodents and non-human primates-through bites, scratches, or handling of carcasses is a major source (Farasani, 2022). Human-tohuman transmission occurs via close contact with lesions, fluids, or respiratory secretions, while contaminated surfaces drive environmental spread. (Upadhayay et al., 2022). The incubation period ranges from 7–14 days, and symptoms include fever, lymphadenopathy, and rash lasting 2–4 weeks. The case fatality rate is 3–6%, with higher risk in immunocompromised individuals (Farahat

et al., 2022). Control measures include isolation of suspected cases, use of PPE, safe carcass handling, and public awareness (Jeyaraman et al., 2022). While no specific cure exists, smallpox vaccination offers ~85% protection, and antiviral drugs such as tecovirimat show promise (Brown & Leggat, 2016).

2.0 METHODS

Mathematical modeling has been widely applied to understand monkey pox (mpox) transmission dynamics and to design control strategies. Recent studies have introduced diverse modeling frameworks addressing human, animal, and environmental transmission, as well as intervention measures. Peter et al. (2023) developed a deterministic compartmental model incorporating human-rodent interactions with quarantine and isolation. Their model, based on an SEIQR structure for humans and SEIR for rodents, analyzed the basic reproduction number R_0 using the next-generation matrix approach and demonstrated local and global stability of the diseasefree equilibrium. Sensitivity analysis identified contact rates and rodent-related parameters as key drivers of infection. Frank (2024) proposed symmetry-based models, such as SIR-SIR and SEIR-SEIR focusing on the concept of "order parameters" derived from eigenvectors to predict outbreak initiation. This approach



WEBSITE: https://fugus-ijsgs.com.ng

ISSNp: 2488-9229; ISSNe: 3027-1118

IJSGS FUGUSAU VOLXXX

provides theoretical insight into threshold dynamics in multi-host systems. In terms of control-oriented modeling, Singo et al. (2024) presented a nonlinear ODE model for Tanzania, evaluating interventions such as vaccination, treatment, and hygiene practices. Their results showed that combined strategies were most effective in reducing R0. Fatoba et al. (2023) proposed an integer-order SITR-SIR model for Nigeria, performing local stability analysis and identifying factors contributing to outbreaks in West Africa.

Finally, Islam et al. (2023) introduced a modified logistic growth model calibrated to the 2022 U.S. outbreak data. This study quantified the impact of non-pharmaceutical interventions on epidemic dynamics and demonstrated the utility of simple models for short-term prediction. These works collectively highlight the importance of incorporating zoonotic, human-to-human, environmental transmission pathways, as well as memory effects and uncertainty, when modeling monkey pox dynamics. They also emphasize the critical role of combined interventions in mitigating outbreak risks. This study develops a mathematical model to explore MPXV dynamics considering human, rodent, and environmental transmission, including contamination, and evaluates strategies to reduce outbreak risk.

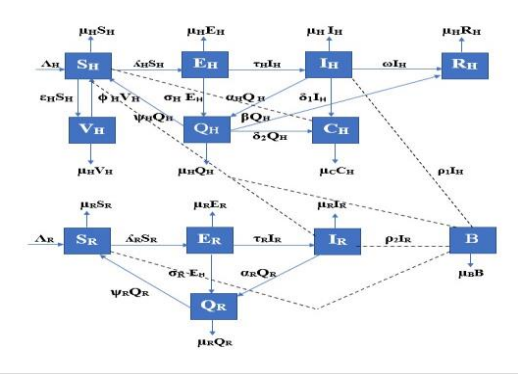


Figure 1: Schematic Diagram of the model

2.1 Description of the MPX disease model

This model describes the MPX disease model. The total human population at time t, is denoted by $N_H(t)$, and is divided into sub-populations of susceptible $S_H(t)$, vaccinated $V_H(t)$, exposed $V_H(t)$, quarantine $V_H(t)$, infectious, $V_H(t)$, carcass, $V_H(t)$, and recovered $V_H(t)$ individuals, such that $V_H(t) = S_H(t) + E_H(t) + Q_H(t) + I_H(t) + R_H(t)$. Also, the total rodent population at time t, denoted by $V_R(t)$, is subdivided into sub-populations of susceptible rodents

 $S_R(t)$, exposed rodents $E_R(t)$, quarantine rodents $Q_R(t)$ and infectious $I_R(t)$ rodents such that $N_R(t) = S_R(t) + E_R(t) + Q_R(t) + I_R(t)$, and environmental contamination compartment B(t).

In order to develop the monkey pox model with carcass compartment, the following assumptions are made: all recruitment occurs via birth or immigration into the population. Susceptible humans can be infected by both infectious rodents and humans. Susceptible human can be infected by carcass. Susceptible humans can be infected via MPXV concentration within the environment due to the shedding of the virus by infectious humans and rodents. Human in MPX endemic areas are vaccinated. The rodents remain infectious and have no recovered class. Individuals either die by infection or natural death and it's also assumed that individuals either die or recovered.

The recruitment of susceptible individuals into the human population occurs via birth or immigration at a constant rate, $\Lambda_{\rm H}$. The susceptible population decreased by vaccination of susceptible humans at a rate, ϵ , while increased through the loss of vaccine-acquired immunity by vaccinated humans, at a waning rate, φ , and through the progression from the quarantine humans, without the symptoms after incubation period, at a rate, ψ . Susceptible humans acquire MPX infection after effective contact with infectious rodents, infectious humans, carcass, and contaminated environment, at a force of infection rate, λ_H is given by

$$\lambda_H = \frac{\beta_1 I_H}{N_H} + \frac{\theta_H \beta_1 C_H}{N_H} + \frac{\beta_2 I_R}{N_R} + \frac{\beta_3 B}{K+B}$$

where β_1 , β_2 and β_3 are transmission rates from infectious humans to susceptible humans, infectious rodents to susceptible humans, and the concentration of MPXV in the environment to susceptible humans, respectively. The parameter, K, is the concentration of MPX pathogen in the environment which increased by 50% to give rise to MPX transmission and B(t) is the environmental contamination compartment. Natural mortality occurs in all human classes at a rate, μ_H so that

$$\frac{dS_H}{dt} = \Lambda_H + \phi_H V_H + \psi_H Q_H - \lambda_H S_H - (\varepsilon_H + \mu_H) S_H$$

The vaccinated human population $V_H(t)$ is formed by the vaccination of susceptible individuals at the rate, \mathcal{E}_H . This population decreases due to the loss of the vaccine at the rate, φ_H , and by the natural death rate, μ_H . This gives



$$\frac{dV_H}{dt} = \varepsilon_H S_H - (\phi_H + \mu_H) V_H$$

The exposed human population $E_H(t)$ is generated by the infection of susceptible humans $S_H(t)$ at the rate, λ_H . The population is decreased by the progression of individuals to the quarantine and infectious compartments at the rates, σ_H and τ_H , respectively, and by the natural death rate, μ_H . This gives,

$$\frac{dE_H}{dt} = \lambda_H S_H - (\sigma_H + \tau_H + \mu_H) E_H$$

The quarantine human population $Q_H(t)$ is formed by the progression of suspected to be exposed humans to the quarantine compartment for observation at a rate, σ_H . This population also decreases by the progression of quarantine individuals without symptoms after incubation period to the susceptible human population at a rate, ψ_H , while those with symptoms are isolated for treatment. Since two things are taking place in the quarantine class, i.e. observation and treatment, the population also increased by the progression of the infectious human that manifested the symptoms to the quarantine class for treatment at the rate, α_H . Also, the population decreases through the recovery of the infected humans at a rate, β_H , and disease induced dead at a rate δ_2 , and by natural death at a rate μ_H . This gives,

$$\frac{dQ_H}{dt} = \sigma_H E_H + \alpha_H I_H - (\psi_H + \beta_H + \delta_2 + \mu_H) Q_H$$

The infectious human population $I_H(t)$ is generated by the progression of exposed human that manifested the symptoms to the infectious compartment at the rates, \mathcal{T}_H . The population decrease by the progression of infectious humans to the quarantine class for treatment not for observation at a rate, \mathcal{C}_H . Also, the population decreases through the natural recovery of the infected humans at a rate ω , and disease induced death (carcass) and natural death at the rate, \mathcal{S}_1 and \mathcal{U}_H . This gives,

$$\frac{dI_H}{dt} = \tau_H E_H - (\alpha_H + \omega_H + \delta_1 + \mu_H) I_H$$

The population of carcass is formed by the death of humans due to the infection in the infectious class and also in the quarantine class i.e. those that are undergoing treatment in the quarantine class at the rate, δ_1 and δ_2

WEBSITE: https://fugus-ijsgs.com.ng

ISSNp: 2488-9229; ISSNe: 3027-1118

respectively, and reduced by proper handling of the carcass at the rate, μ_C so that

$$\frac{dC_H}{dt} = \delta_1 I_H + \delta_2 Q_H - \mu_C C_H$$

The recovered human population is formed by the natural recovery of infectious humans at the rate, ω_H , and the recovery of those undergoing treatment in the quarantine class at the rate, β_H , and reduces by the natural death at the rate, μ_H so that

$$\frac{dR_H}{dt} = \omega_H I_H + \beta_H Q_H - \mu_H R_H$$

The class of susceptible rodents $S_R(t)$ is recruited at a constant rate, Λ_R , and is increased by progression from quarantine rodents without symptoms after an incubation period at a rate, ψ_R . It is also decreased by infection following significant contact with infectious rodents at a rate, λ_R , where,

$$\lambda_R = \frac{\beta_4 I_R}{N_R} + \frac{\theta_R \beta_3 B}{K + B}$$

where the transmission rate between susceptible and infectious rodents is denoted by β_4 . In all rodent compartments, natural mortality happens at a rate, μ_R . This yield,

$$\frac{dS_R}{dt} = \Lambda_R + \psi_R Q_H - (\lambda_R S_R + \mu_R) S_R$$

The exposed Rodent population $E_R(t)$ is formed by the infection of susceptible rodents $S_R(t)$ at the rate, λ_R . This population is reduced by the progression of the rodent to the quarantine and infectious compartments at the rates, σ_R and τ_R , respectively, and by the natural death rate, μ_R . Thus,

$$\frac{dE_R}{dt} = \lambda_R S_R - (\sigma_R + \tau_R + \mu_R) E_R$$

The quarantine rodent population $Q_R(t)$ is generated by the progression of suspected to be exposed Rodents to the quarantine compartment for observation at a rate, σ_R . This population also decreases with the progression of quarantine rodent without symptoms after incubation period to the susceptible class at a rate, ψ_R , while those with symptoms are isolated to restrict their movement and implementing control measures to prevent further spread of the virus. The population also increased by the progression of infectious rodent that missed the

IJSGS FUGUSAU VOLXXX

quarantine strategy to the quarantine class at a rate, α_R , and decreased by natural death at a rate, μ_R This gives,

$$\frac{dQ_R}{dt} = \sigma_R E_R + \alpha_R I_R - (\psi_R + \mu_R) Q_R$$

The infectious rodent population $I_R(t)$ is formed by the progression of exposed rodent that manifested the signs and symptoms to the infectious compartment at the rates, τ_R . The population decreased by the progression of infectious rodent to the quarantine class to restrict their movement and implement a control measures at a rate, α_R , respectively. This gives,

$$\frac{dI_R}{dt} = \tau_R E_R - (\alpha_R + \mu_R) I_R$$

MPXV concentrations in the environment are produced when the infected humans and rodents shed the virus in the environment at the rates, $\,
ho_1 \,$ and $\,
ho_2 \,$, and decreased by the decay of the virus in the environment at a rate, $\mu_{\rm B}$

$$\frac{dB}{dt} = \rho_1 I_H + \rho_2 I_R - \mu_B B$$

Thus, the full system of equations for the transmission dynamics of the MPX disease is given by the following nonlinear system of differential equations,

WEBSITE: https://fugus-ijsgs.com.ng

$$\frac{dS_H}{dt} = \Lambda_H + \phi_H V_H + \psi_H Q_H - \lambda_H S_H - (\varepsilon_H + \mu_H) S_H
\frac{dV_H}{dt} = \varepsilon_H S_H - (\phi_H + \mu_H) V_H
\frac{dE_H}{dt} = \lambda_H S_H - (\sigma_H + \tau_H + \mu_H) E_H
\frac{dQ_H}{dt} = \sigma_H E_H + \alpha_H I_H - (\psi_H + \beta_H + \delta_2 + \mu_H) Q_H
\frac{dI_H}{dt} = \tau_H E_H - (\alpha_H + \omega_H + \delta_1 + \mu_H) I_H
\frac{dC_H}{dt} = \delta_1 I_H + \delta_2 Q_H - \mu_C C_H
\frac{dR_H}{dt} = \omega_H I_H + \beta_H Q_H - \mu_H R_H
\frac{dS_R}{dt} = \lambda_R S_R - (\sigma_R + \tau_R + \mu_R) S_R
\frac{dE_R}{dt} = \lambda_R S_R - (\sigma_R + \tau_R + \mu_R) E_R
\frac{dQ_R}{dt} = \sigma_R E_R + \alpha_R I_R - (\psi_R + \mu_R) Q_R
\frac{dI_R}{dt} = \tau_R E_R - (\alpha_R + \mu_R) I_R
\frac{dB}{dt} = \rho_1 I_H + \rho_2 I_R - \mu_B B$$
(1)

with the initial condition

$$\begin{split} S_H(0) > 0, V_H(0) \ge 0, \ E_H(0) \ge 0, \ Q_H(0) \ge 0, \ I_H(0) \ge 0, \ C_H(0) \ge 0, \ R_H(0) \ge 0 \\ S_R(0) > 0, \ E_R(0) \ge 0, \ Q_R(0) \ge 0, \ I_R(0) \ge 0, \ B(0) \ge 0 \end{split}$$

Table 1: Description of the State Variables of the Model

Variables	Description			
$S_H(t)$	Susceptible Human Population at time t .			
$V_H(t)$	Vaccinated Human Population at time t .			
$E_H(t)$	Exposed Human Population at time t .			
$Q_H(t)$	Quarantined Human Population at time t .			
$I_H(t)$	Infected Human Population at time t .			
$C_H(t)$	Carcass at time t .			
$R_H(t)$	Recovered Human Population at time $t.$			
$S_R(t)$	Susceptible Rodent Population at time t .			
$E_R(t)$	Exposed Rodent Population at time t .			
$Q_{R}(t)$	Quarantined Rodent Population at time $t.$			



IJSGS FUGUSAU VOLXXX				
$I_R(t)$	Infected Rodent Population at time t .			
B(t)	Environmental contamination at time t .			

Table 2: Parai	meters description of the model
Parameters	Description
$\Lambda_{\scriptscriptstyle H}$	The human constant recruitment rate.
$\lambda_{_{\! H}}$	Force of infection for human.
$\mu_{\scriptscriptstyle H}$	Natural death rate.
$\mu_{\scriptscriptstyle C}$	The rate at which carcasses are properly handled.
$ au_{\scriptscriptstyle H}$	The rate of progression from exposed to infected humans.
$\psi_{\scriptscriptstyle H}$	The progression rate from quarantine to susceptible humans.
\mathcal{O}_H	The natural recovery rate from infected to recovered.
$eta_{\scriptscriptstyle H}$	The recovery rate from quarantine to recovered humans.
\mathcal{E}_H	The rate of transmission from susceptible to vaccinated human.
$\phi_{\scriptscriptstyle H}$	The rate at which vaccine failed from the vaccinated to susceptible human.
$\sigma_{\scriptscriptstyle H}$	The rate of transmission from susceptible to quarantined human.
$lpha_{_H}$	The progression rate from infected to quarantine humans.
$\delta_{_{1}}$	The rate of movement from infected human to carcass.
$\delta_{\scriptscriptstyle 2}$	The rate of movement from quarantined human to carcass.
$oldsymbol{eta}_{\!\scriptscriptstyle 1}$	Human to human contact rate.
$oldsymbol{eta}_2$	Rodent to human contact rate.
$ heta_{\!\scriptscriptstyle H} \ eta_{\!\scriptscriptstyle 3}$	The modification parameter that rate of infectiousness in human. Environmental transmission rate.
$oldsymbol{eta_3}{oldsymbol{eta_4}}$	Rodent to rodent contact rate.
K	Concentration of the disease pathogen in the environment.
$\mu_{\!\scriptscriptstyle B}$	Decay rate of monkey pox virus in the environment.
$ ho_{\scriptscriptstyle 1}$	Shedding rate of infectious humans to the environment.
$ ho_2$	Shedding rate of infectious rodents to the environment. The rodent constant recruitment rate.
$egin{array}{c} \Lambda_{_R} \ \lambda_{_R} \end{array}$	Force of infection for the rodents.
$\mu_{_R}$	Natural death rate for the rodents
τ_R	The rate of transmission from exposed to
$\sigma_{_R}$	infected human. The rate of transmission from susceptible to quarantined rodents.

WEBSITE: https://fugus-ijsgs.com.ng					
$\theta_{\scriptscriptstyle R}$	The modification parameter that rate of infectiousness in rodents.				
ψ_R	The rate of progression from quarantined to susceptible rodent.				
$\alpha_{\scriptscriptstyle R}$	The rate of progression from infected to				

ISSNp: 2488-9229; ISSNe: 3027-1118

3.0 BASIC PROPERTIES OF MPX MODEL 3.1 Invariant region of MPX model

The study of the invariant region is carried-out to determine whether the solutions of the model system (1) make biological sense. To obtain this, first we considered the total Human population N_{H} , followed by the Rodent population, N_R .

$$N_{H} = S_{H}(t) + V_{H}(t) + E_{H}(t) + Q_{H}(t) + I_{H}(t) + R_{H}(t)$$

Then, differentiating N_H both sides of equation (2)

with respect to t and simplifying leads to

$$\frac{dN_H}{dt} = \Lambda_H - \mu_H N_H - \delta_u H_u - \mu_C C_H$$

Also for the rodent population, we have

$$N_{R} = S_{R}(t) + E_{R}(t) + Q_{R}(t) + I_{R}(t)$$
 (4)

While differentiating N_R both sides of equation (3)

with respect to t and simplifying leads to

$$\frac{dN_R}{dt} = \Lambda_R - \mu_R N_R \tag{5}$$

Therefore, the total population of the system (1) is given

$$\frac{dN_{H}}{dt} = \Lambda_{H} - \mu_{H} N_{H} - \alpha_{A}^{H} I_{A}^{H} - \alpha_{S}^{H} I_{S}^{H}$$

$$\frac{dN_{R}}{dt} = \Lambda_{R} - \mu_{R} N_{R}$$

$$\frac{dB}{dt} = \rho_{1} I_{H} + \rho_{2} I_{R} - \mu_{B} B$$
(6)

In the absence of disease-induced death, the Human and Rodent populations can be simplified as:

$$\frac{dN_{H}}{dt} = \Lambda_{H} - \mu_{H} N_{H}
\frac{dN_{R}}{dt} = \Lambda_{R} - \mu_{R} N_{R}$$
(7)



IJSGS FUGUSAU VOLXXX

Theorem 1: The closet

$$\Omega_{H} = \left\{ X \in \mathbb{R}^{12}_{+}; N_{H} \leq \frac{\Lambda_{H}}{\mu_{H}}, B \leq \frac{(\rho_{1}I_{H} + \rho_{2}I_{R})}{\mu_{B}}, N_{R} \leq \frac{\Lambda_{R}}{\mu_{R}} \right\} \frac{dB}{dt} = \rho_{1}I_{H} + \rho_{2}I_{R} - \mu_{B}B$$

is positively invariant and attracting with respect to the model(1).

Proof:

In the absence of disease-induced death, (i.e.

$$\delta_u = \delta_{qu} = 0$$
), and by comparison theorem, equation

(3) becomes

$$\frac{dN_{_H}}{dt} \leq \Pi - \mu_{_H} N_{_H}$$

Solving equation (8) by method of integrating factor and applying initial condition resulted into

$$N_H(t) \le \frac{\Lambda_H}{\mu_H} + \left(N_H(0) - \frac{\Lambda_H}{\mu_H}\right) e^{-\mu_H t}$$

(9)

Further simplification of equation (9) resulted into

$$N_H(t) \le N_H(0)e^{-\mu_H t} + \frac{\Lambda_H}{\mu_H} (1 - e^{-\mu_H t})$$

From equation (10), it can be observed that $N_H(t) \rightarrow \left(\frac{\Lambda_H}{\mu_U}\right)$ as $t \rightarrow \infty$. That is, the total population

size $N_{H}(t)$ takes off from the value $N_{H}(0)$ at the initial time t = 0 and ends up with the bounded value Λ_H as

the time t grows to infinity. Thus, it can be concluded that $N_H(t)$ is bounded within $0 \le N_H(t) \le \frac{11}{U}$.

Applying the same approach to the Rodent population, it can be observed that

$$N_R(t) = N_R(0)e^{-\mu_R t} + \frac{\Lambda_R}{\mu_R} (1 - e^{-\mu_R t})$$

(11)

From equation (4.35), it can be observed that $N_R(t) \rightarrow \left(\frac{\Lambda_R}{\mu_R}\right)$ as $t \rightarrow \infty$. That is, the total population

size $N_{R}(t)$ takes off from the value $N_{R}(0)$ at the initial time t = 0 and ends up with the bounded value Λ_R as

the time t grows to infinity. Thus, it can be concluded that $N_R(t)$ is bounded within $0 \le N_A(t) \le \frac{\Lambda_A}{\mu_A}$.

Similarly, the equation of the contaminated environment

WEBSITE: https://fugus-ijsgs.com.ng

$$\frac{dB}{dt} = \rho_1 I_H + \rho_2 I_R - \mu_B B \tag{12}$$

Resolving equation (12), we have

$$B(t) \le B(0)e^{-\mu_B t}$$

This shows that as $t \to \infty$, $B(t) \to B(0)$

Thus, the feasible solution set of the system (1) of the model enters and remains in the region:

$$\Omega_H = \left\{ X \in \mathbb{R}^{12}_+; N_H \leq \frac{\Lambda_H}{\mu_H}, B(t) \leq B(0)e^{-\mu_B t}, N_R \leq \frac{\Lambda_R}{\mu_R} \right\},$$

Hence, our MPX model is well posed and biologically meaningful.

3.2 Positivity of the solution for the MPX model

In this section, it was shown that all the solutions of the model equation (1) remain positive for future time if their respective initial values are positive. Since the model monitors humans and rodent population, it's significant to show that all the state variables in the model is non negative for all time.

Theorem 2: For non-negative initial conditions of the system (1)

 $\{(S_H(0), V_H(0), E_H(0), Q_H(0), I_H(0), R_H(0), S_R(0), E_R(0), Q_R(0), I_R(0), E_R(0), I_R(0), E_R(0), I_R(0), E_R(0), I_R(0), E_R(0), I_R(0), E_R(0), E_R(0), I_R(0), E_R(0), E_$

 $S_{H}(t), V_{H}(t), E_{H}(t), Q_{H}(t), I_{H}(t), R_{H}(t), S_{R}(t), E_{R}(t), Q_{R}(t), I_{R}(t), B(t)$ of the model equations (1) are all non-negative for all time, $t \ge 0$.

Proof: For the equations of the system (1), let t_1 be the maximum time of the epidemics. This implies that;

$$t_1 = \sup\{t > 0: S > 0, V > 0, E_u > 0, E_v > 0, H_u > 0, H_A > 0, H_v > 0, Q_u > 0, H_u > 0,$$

Thus, $t_1 \ge 0$. Then it follows from the first equation of the system (1), we obtain from the equation of the susceptible humans, we have

$$\frac{dS_H}{dt} = -(\lambda_H + \varepsilon + \mu_H)S_H \ge -(\lambda_H + (\varepsilon_H + \mu_H))S_H$$

Applying method of separable variable on equation (13), we have

$$\frac{dS_H}{S_H} \ge -(\lambda_H(z)dz + (\varepsilon_H + \mu_H))dt_1 > 0$$

Integrating equation (14) and simplifying, we get



WEBSITE: https://fugus-ijsgs.com.ng

IJSGS FUGUSAU VOLXXX

$$S_{H}(t_{1}) \ge S_{H}(0)e^{-\int_{0}^{t_{1}} \lambda_{H}(z)dz - (\varepsilon_{H} + \mu_{H})t_{1}} > 0$$
(15)

Using the same argument, it can be shown that the other state variables: $V_H(t)$, $E_H(t)$, $Q_H(t)$, $I_H(t)$, $R_H(t)$, $S_R(t)$, $E_R(t)$, $Q_R(t)$, $I_R(t)$, B(t), are all positive for time $t_1 > 0$. thus, the solutions of (1) remain positive for all $t_1 \ge 0$.

3.3 Equilibrium states

At equilibrium state, the rate of change of all the state variables are equal to zero. That is

$$\frac{dS_H}{dt} = \frac{dV_H}{dt} = \frac{dE_H}{dt} = \frac{dQ_H}{dt} = \frac{dI_H}{dt} = \frac{dR_H}{dt} = \frac{dS_R}{dt} = \frac{dE_R}{dt} = \frac{dQ_R}{dt}$$
(16)

Thus, at equilibrium state, substituting the model equations into equation (16), gives

$$\begin{split} &\Lambda_{H} + \phi_{H}V_{H} + \psi_{H}Q_{H} - \lambda_{H}S_{H} - (\varepsilon_{H} + \mu_{H})S_{H} = 0 \\ &\varepsilon_{H}S_{H} - (\phi_{H} + \mu_{H})V_{H} = 0 \\ &\lambda_{H}S_{H} - (\sigma_{H} + \tau_{H} + \mu_{H})E_{H} = 0 \\ &\sigma_{H}E_{H} + \alpha_{H}I_{H} - (\psi_{H} + \beta_{H} + \delta_{2} + \mu_{H})Q_{H} = 0 \\ &\tau_{H}E_{H} - (\alpha_{H} + \omega_{H} + \delta_{1} + \mu_{H})I_{H} = 0 \\ &\delta_{1}I_{H} + \delta_{2}Q_{H} - \mu_{C}C_{H} = 0 \\ &\omega_{H}I_{H} + \beta_{H}Q_{H} - \mu_{H}R_{H} = 0 \\ &\Lambda_{R} + \psi_{R}Q_{H} - (\lambda_{R}S_{R} + \mu_{R})S_{R} = 0 \\ &\lambda_{R}S_{R} - (\sigma_{R} + \tau_{R} + \mu_{R})E_{R} = 0 \\ &\sigma_{R}E_{R} + \alpha_{R}I_{R} - (\psi_{R} + \mu_{R})Q_{R} = 0 \\ &\tau_{R}E_{R} - (\alpha_{R} + \mu_{R})I_{R} = 0 \\ &\rho_{1}I_{H} + \rho_{2}I_{R} - \mu_{B}B = 0 \\ &(17) \end{split}$$

where

$$\lambda_H = \frac{\beta_1 I_H}{N_H} + \frac{\theta_H \beta_1 C_H}{N_H} + \frac{\beta_2 I_R}{N_R} + \frac{\beta_3 B}{K+B} \quad , \quad \lambda_R = \frac{\beta_4 I_R}{N_R} + \frac{\theta_R \beta_3 B}{K+B}$$

3.4 Disease free equilibrium state

(18)

The modified MPX-free equilibrium point is steady-state solution where there is no MPX infection in the population. Thus, in the absence of MPX, we set infectious states to zero,

$$E_H = Q_H = I_H = C_H = R_H = E_R = R_H = E_R = Q_R = I_R = B \neq 0$$
(20)

Where,

. Equations of the system (1) are solved simultaneously and therefore, the MPX-free equilibrium point is obtained, hence,

$$E_0 = \left\{ \frac{\Lambda_H(\phi_H + \mu_H)}{\mu_H(\varepsilon_H + \phi_H + \mu_H)}, \frac{\varepsilon_H \Lambda_H}{\mu_H(\varepsilon_H + \phi_H + \mu_H)}, 0, 0, 0, 0, 0, \frac{\Lambda_R}{\mu_R}, 0, 0, 0, 0 \right\}$$

$$(19)$$

3.5 Endemic equilibrium state

The MPX endemic equilibrium points are steady-state solution where MPX Viral infection persists in the population. At endemic equilibrium, the infectious states are not equal to zero, $E_H \neq 0, Q_H \neq 0, I_H \neq 0, C_H \neq 0, R_H \neq 0, E_R \neq 0, R_H \neq 0, E_R \neq 0, Q_R \neq 0, I_R \neq 0, B \neq 0$

dITo establish the existence of endemic equilibria of our MPX mod θ , we solve equations of the system (17-28) at steady state simultaneously.

where the force of infection is as defined in equation (29)

$$S_{H}^{*} = \frac{\Lambda_{H} + \phi_{H} V_{H}^{*} + \psi_{H} Q_{H}^{*}}{M_{1}}$$

$$V_H^* = \frac{\varepsilon_H (\Lambda_H + \phi_H V_H^* + \psi_H Q_H^*)}{M_1 M_2}$$

$$E_{H}^{*} = \frac{\lambda_{H}^{*} (\Lambda_{H} + \phi_{H} V_{H}^{*} + \psi_{H} Q_{H}^{*})}{M_{1} M_{3}}$$

$$Q_{H}^{*} = \frac{M_{1}M_{3}\alpha_{H}I_{H}^{*} + \sigma_{H}\lambda_{H}^{*}(\Lambda_{H} + \phi_{H}V_{H}^{*} + \psi_{H}Q_{H}^{*})}{M_{1}M_{2}M_{4}}$$

$$I_{H}^{*} = \frac{\tau_{H}\lambda_{H}^{*}(\Lambda_{H} + \phi_{H}V_{H}^{*} + \psi_{H}Q_{H}^{*})}{M_{1}M_{3}M_{5}}$$

$$C_{H}^{*} = \frac{M_{1}M_{3}M_{5} + \delta_{1}\tau_{H}\lambda_{H}^{*}(\Lambda_{H} + \phi_{H}V_{H}^{*} + \psi_{H}Q_{H}^{*})}{\mu_{C}M_{1}M_{3}M_{5}}$$

$$R_{H}^{*} = \frac{M_{1}M_{3}M_{5} + \omega_{H}\tau_{H}\lambda_{H}^{*}(\Lambda_{H} + \phi_{H}V_{H}^{*} + \psi_{H}Q_{H}^{*})}{\mu_{H}M_{1}M_{3}M_{5}}$$

$$S_R^* = \frac{\Lambda_R + \psi_R Q_R^*}{M_C}$$

$$E_R^* = \frac{\lambda_R^* (\Lambda_R + \psi_R Q_R^*)}{M M}$$

$$Q_{R}^{*} = \frac{M_{6}M_{9}\alpha_{R}I_{R}^{*} + \sigma_{R}\lambda_{R}^{*}(\Lambda_{R} + \psi_{R}Q_{R}^{*})}{M_{6}M_{7}M_{9}}$$

$$I_R^* = \frac{\tau_R \lambda_R^* (\Lambda_R + \psi_R Q_R^*)}{M_6 M_7 M_9}$$

$$B^* = \frac{1}{\mu_B} \left(\frac{\rho_1 \tau_H \lambda_H^* (\Lambda_H + \phi_H V_H^* + \psi_H Q_H^*)}{M_1 M_3 M_5} + \frac{\rho_2 \tau_R \lambda_R^* (\Lambda_R + \psi_R Q_R^*)}{M_6 M_7 M_9} \right)$$

IJSGS FUGUSAU VOLXXX

WEBSITE: https://fugus-ijsgs.com.ng

$$M_{1} = (\varepsilon_{H} + \lambda_{H} + \mu_{H}), M_{2} = (\phi_{H} + \mu_{H}), M_{3} = (\sigma_{H} + \tau_{H} + \mu_{H}), M_{4} = (\psi_{H} + \beta_{H} + \delta_{2} + \mu_{H})$$

$$M_{5} = (\alpha_{H} + \omega_{H} + \delta_{1} + \mu_{H}), M_{6} = (\lambda_{R} + \mu_{R}), M_{7} = (\sigma_{R} + \tau_{R} + \mu_{R}), M_{8} = (\psi_{R} + \mu_{R}), M_{9} = (\alpha_{R} + \mu_{R})$$

4.0 Basic Reproduction Number

This section studies the effective reproduction number, which is a threshold parameter that controls the spread of a disease. To obtain the effective reproduction number, we apply the next generation approach described in (Van den 2002). The associated incidence term F_m and the transfer term V_m for the MPX model was obtained.

Thus, the effective reproductive number of system model (1) is calculated from the spectral radius $\rho(FV^{-1})$ as: Therefore, the basic reproduction number, R_0 for the monkey pox virus model is given by

$$R_0 = \rho F V^{-1} = \max \{R_{0R}, R_{0H}\}$$

where

$$R_{0R} = \frac{\tau_R \theta_R \beta_3 \Lambda_R (\psi_R + \beta_H + \delta_2 + \mu_H) + \tau_R \mu_B \beta_4}{K \mu_R^2 (\sigma_R + \tau_R + \mu_R) (\alpha_R + \mu_R)}, \quad R_{0R} = \frac{\theta_H \beta_1 \mu_H (\phi_H + \mu_H) \delta_2 \sigma_H}{\mu_H (\psi_H + \beta_H + \delta_2 + \mu_H) (\varepsilon_H + \phi_H + \mu_H) (\alpha_R + \mu_R)}$$
(21)

where the reproduction numbers for transmission from human to human and from rodent to rodent are, respectively, R_{0R} and R_{0H} .

when $R_{0R} < 1$, $R_{0H} < 1$, the monkey pox infection can be eradicated in both the rodent and human host populations, but it can continue in both when $R_{0R} > 1$, $R_{0H} > 1$, as demonstrated by Diekmann and Heesterbeek, (2002).

4.1 Local Stability of monkey pox Free Equilibrium

Lemma 1: The Disease-free equilibrium point E_{θ} is locally asymptotically stable if $R_{\theta} < l$ and unstable whenever $R_{\theta} > l$, (Akinyemi et al., 2018)

4.2 Global Stability of Monkey pox Free Equilibrium

In this section, the global stability of the disease free equilibrium for the model (1) was investigated using the theorem by (Castillo-Chavez and Song, 2004)

Lemma 2: Consider a model system written in the form

$$\frac{dY}{dt} = F(Y,Z)$$

$$\frac{dZ}{dt} = G(Y,Z), (Y,0) = 0$$
(22)

where $Y = (S_H, V_H, R_H, S_R)$ and $Z = (E_H, Q_H, I_H, C_H, E_R, I_R, B)$ with the components of $Y \in \mathbb{R}^4$ denoting the uninfected population and the components of $Z \in \mathbb{R}^7$ denoting infected population.

The disease free equilibrium is now denoted as:

$$E_0 = \left\{ \frac{\Lambda_H(\phi_H + \mu_H)}{\mu_H(\varepsilon_H + \phi_H + \mu_H)}, \frac{\varepsilon_H \Lambda_H}{\mu_H(\varepsilon_H + \phi_H + \mu_H)}, 0, 0, 0, 0, 0, \frac{\Lambda_R}{\mu_R}, 0, 0, 0, 0, 0 \right\}$$

The two conditions to be met for global asymptotic stability are:

i.
$$\frac{dY}{dt} = F(Y,0)$$
, E_0 is globally asymptotically stable (GAS).

ii.
$$(H_2)$$
. $G(Y,Z) = AZ - \hat{G}(Y,Z), \hat{G}(Y,Z) \ge 0$,

where $P = D_z G(X^0, 0)$ is a M-matrix (the off-diagonal elements of P are non-negative) and Ω is the region where the model makes biological sense. Then, the DFE X_0 is globally asymptotically stable provided that $R_0 < 1$ (Castillo-Chavez et al. 2002)

Theorem 3: The MPX- free equilibrium point $E_0 = (Y^0, 0)$ of the system model (1) is globally asymptotically stable provided $R_0 < 1$ and the conditions (H1) and (H2) are satisfied.

Proof: from the model (1) we can get F(Y,Z) and G(Y,Z)



LISGS FUGUSAU VOLXXX

WEBSITE: https://fugus-ijsgs.com.ng

Evaluating at MPX free equilibrium

$$F(Y,0) = \begin{pmatrix} \Lambda_H + \phi_H V_H - (\varepsilon_H + \mu_H) S_H \\ \varepsilon_H S_H - (\phi_H + \mu_H) V_H \\ 0 \\ \Lambda_R - \mu_R S_R \end{pmatrix}$$
(23)

Thus,

as $t \to \infty$. Since the solution (83) converges, therefore, E_{θ} is globally asymptotically stable. Condition II

$$G(Y,Z) = AZ - \hat{G}(Y,Z), \hat{G}(Y,Z) \ge 0, \text{ for } (Y,Z) \in \Omega$$
 (24)

and $A=D_IG(Y^*,0)$ is an M-matrix (the off-diagonal elements of are nonnegative) with respect to Z, where $Z=(E_H,Q_H,I_H,C_H,E_R,I_R,B)$ such that

$$A = \begin{pmatrix} -w_0 & 0 & \frac{\beta_1 S_H^0}{N_H^0} & \frac{\beta_1 \theta_H S_H^0}{N_H^0} & 0 & 0 & \frac{\beta_2 S_H^0}{N_R^0} & \frac{\beta_3 S_H^0}{K} \\ \sigma_H & -w_1 & \alpha_H & 0 & 0 & 0 & 0 & 0 \\ \tau_H & 0 & -w_2 & 0 & 0 & 0 & 0 & 0 \\ 0 & \delta_2 & \delta_1 & -\mu_c & 0 & 0 & 0 & 0 \\ 0 & 0 & 0 & 0 & -w_3 & 0 & \frac{\beta_4 S_R^0}{N_R^0} & \frac{\theta_R \beta_3 S_R^0}{K} \\ 0 & 0 & 0 & 0 & \sigma_R & -w_4 & \alpha_R & 0 \\ 0 & 0 & 0 & 0 & \tau_R & 0 & -(\alpha_R + \mu_R) & 0 \\ 0 & 0 & \rho_1 & 0 & 0 & 0 & \rho_2 & -\mu_B \end{pmatrix}$$
 (25)

where

$$w_0 = (\sigma_H + \tau_H + \mu_H), w_1 = (\psi_H + \beta_H + \mu_H), w_2 = (\alpha_H + \omega_H + \mu_H), w_3 = (\sigma_R + \tau_R + \mu_R), w_4 = (\psi_R + \mu_R)$$

So that,

$$AZ = \begin{pmatrix} \frac{\beta_{1}S_{H}^{0}I_{H}}{N_{H}^{0}} - (\sigma_{H} + \tau_{H} + \mu_{H})E_{H} + \frac{\beta_{2}S_{H}^{0}I_{R}}{N_{R}^{0}} + \frac{\beta_{3}BS_{H}^{0}}{K} + \frac{\beta_{1}\theta_{H}S_{H}^{0}C_{H}}{N_{H}^{0}} \\ \sigma_{H}E_{H} + \alpha_{H}I_{H} - (\psi_{H} + \beta_{H} + \delta_{2} + \mu_{H})Q_{H} \\ \tau_{H}E_{H} - (\alpha_{H} + \omega_{H} + \delta_{1} + \mu_{H})I_{H} \\ \delta_{1}I_{H} + \delta_{2}Q_{H} - \mu_{C}C_{H} \\ \frac{\beta_{4}S_{H}^{0}I_{R}}{N_{R}^{0}} - (\sigma_{R} + \tau_{R} + \mu_{R})E_{R} + \frac{\beta_{3}BS_{H}^{0}\theta_{R}}{K} \\ \sigma_{R}E_{R} + \alpha_{R}I_{R} - (\psi_{R} + \mu_{R})Q_{R} \\ \tau_{R}E_{R} - (\alpha_{R} + \mu_{R})I_{R} \\ \rho_{1}I_{H} + \rho_{2}I_{R} - \mu_{R}B \end{pmatrix}$$

$$(26)$$

Therefore,



WEBSITE: https://fugus-ijsgs.com.ng

$$\begin{pmatrix}
\beta_{1}I_{H} + \theta_{H}\beta_{1}C_{H} + \frac{\beta_{2}\mu_{R}I_{R}}{\Lambda_{R}} + \frac{\beta_{3}B}{K} \end{pmatrix} \begin{pmatrix}
S_{H}^{0} - \frac{S_{H}^{0}}{N_{H}} \end{pmatrix} \\
0 \\
0 \\
0 \\
(27)$$

$$\begin{pmatrix}
\beta_{4}I_{R} + \frac{\theta_{R}\beta_{3}\Lambda_{R}B}{\mu_{R}} \end{pmatrix} \begin{pmatrix}
1 - \frac{S_{R}^{0}}{N_{R}} \end{pmatrix} \\
0 \\
0 \\
0
\end{pmatrix}$$

In the $\operatorname{region}\Omega$, $S_H^0 \leq N_H$. Hence, if the Human and Rodents population is at equilibrium level, then we

have
$$(S_{\scriptscriptstyle H}^{\scriptscriptstyle 0} - \frac{S_{\scriptscriptstyle H}^{\scriptscriptstyle 0}}{N_{\scriptscriptstyle H}}) > 0$$
 and $(1 - \frac{S_{\scriptscriptstyle R}^{\scriptscriptstyle 0}}{N_{\scriptscriptstyle R}}) > 0$

Therefore, $\hat{G}(Y,Z) \ge 0$. Hence the second condition is satisfied.

5.0 Sensitivity Analysis of MPX Model

In this section, we are going to provide the monkey pox virus model's sensitivity analysis. In order to conduct the analysis, we used the method described by (Blower and Dowlatabadi, 1994). This technique develops a formula to obtain the sensitivity index of all the basic parameters defined as:

$$\Delta_x^{R_0} = \frac{\partial R_0}{\partial x} \times \frac{x}{R_0}$$
, where x represents all the basic parameters.

Therefore,

For
$$\beta_1$$
, $\nabla_{\beta_1}^{R_0} = \frac{\partial R_0}{\partial \beta_1} \times \frac{\beta_1}{R_0}$ (28)

$$\frac{\partial R_0}{\partial \beta_1} = \frac{\partial \left(\frac{\sigma_H \beta_1 \mu_H (\phi_H + \mu_H) \phi_2 \sigma_H}{\mu_H (\epsilon_H + \phi_H + \mu_H) (\sigma_H + \tau_H + \mu_H) (\psi_H + \beta_H + \delta_2 + \mu_H)} \right)}{\partial \beta_1} \tag{29}$$

and

$$\frac{\beta_1}{R_0} = \frac{\beta_1}{\left(\frac{\theta_H \beta_1 \mu_H (\phi_H + \mu_H) \delta_2 \sigma_H}{\mu_H (\epsilon_H + \phi_H + \mu_H) (\sigma_H + \tau_H + \mu_H) (\psi_H + \beta_H + \delta_2 + \mu_H)}\right)}$$

The same approach is applied to the remaining parameters to obtain the results for all parameters. The results of the analysis are presented in Table 3.

Table 3: Sensitivity indices for MPXV reproduction number **Parameter Baseline values** Sensitivity index R_{0R} Sensitivity index R_{0H} 8000 Λ_H 0.029 λ_H 0.2 0.00041 -2.0543 μ_H 0.04 μ_C 0.2 -0.0833 τ_H 2.0 0.4396 -0.6192 ψ_H 0.83 ω_H 0.93 0.1078 -0.2879 β_H



ISSNp: 2488-9229; ISSNe: 3027-1118

IJSGS FUGUSAU VOLXXX		WEBSITE: https://fugus-ijsgs.com.ng		
ϵ_H	0.1-1	-	-0.8715	
ϕ_H	0.095	-	0.0815	
σ_H	2.0	-	0.1667	
α_H	0.52	-	-	
δ_1	0.1	-	-	
δ_2	0.1	0.1106	0.9690	
$oldsymbol{eta}_1$	0.000063	-	1	
β_2	0.00025	-	-	
θ_H	0.03	-	1	
$oldsymbol{eta}_3$	0.01	0.2419	-	
eta_4	0.27	0.2005	-	
K	500	-1.0	-	
μ_B	0.003	0.2005	-	
$ ho_1$	0.04	-	-	
ρ_2	0.02	-	-	
Λ_R	0.2	0.7995	-	
λ_R	0.03	-	-	
μ_R	0.3	-3.9286	-	
Tr	0.3	0.3535	-	
σ_R	0.4	-0.4	-	
$ heta_R$	0.5	0.7995	-	
ψ_R	1.0	-	-	
α_R	0.4	-05714	<u>-</u>	

The parameters

 ψ_H , σ_H , α_H , δ_2 , β_3 , β_4 , μ_B and θ_R , exhibits positive sensitivity indices. And the parameters τ_H , ϵ_H , K, μ_R , $\sigma_R \alpha_R$ exhibits negative sensitivity indices. Therefore, the sensitivity indices evaluated in relation to the basic reproduction number of the parameters are organized in Tables (3). Those parameters that have positive indices shows that they have great impact in spreading the infection in the community if their values are increasing. Conversely, those parameters in which their sensitivity indices are negative have an influence of reducing the burden of the disease in the community if their values increase.

6. 0 NUMERICAL SIMULATIONS

In this section, the values in Tables 3 and Table 4 are used to perform numerical simulation on the system of equations. Simulations were run on the following subpopulation dynamics: subpopulation dynamics plotted against time, subpopulation dynamics plotted against time with varied β_1 , subpopulation dynamics plotted against time with varied β_4 . This study aims to investigate the effects of the monkeypox virus on the populace and identify the most effective means of controlling the virus's spread among humans.

Table 3: Initial values used in the model

Variables	Values	Reference	Variables	Values	Reference
S_H	8000	Madubueze et al., (2022)	R_H	2000	Usman and Adamu (2017)
V_H	5000	Madubueze et al., (2022)	S_R	250	Usman and Adamu (2017)
E_H	400	Assumed	E_R	125	Usman and Adamu (2017)
Q_H	100	Madubueze et al., (2022)	Q_R	80	Assumed
I_H	2000	Usman and Adamu (2017)	I_R	100	Madubueze et al., (2022)
C_H	300	Assumed	В	50	Madubueze et al., (2022)



0.3

ISSNp: 2488-9229; ISSNe: 3027-1118

IJSGS FUGUSAU VOLXXX			WEBSITE: https://fugus-ijsgs.com.ng		
Parameter	Values	Reference	Parameter	Values	Reference
Λ_H	800	Madubueze et al., (2022)	ϵ_H	0.1-1	Emeka et al. (2018)
μ_H	0.2	Usman and Adamu (2017)	ϕ_H	0.095	Usman and Adamu (2017)
μ_C	0.04	Assumed	σ_H	2.0	Peter et al. (2022)
$ au_H$	0.2	Peter et al. (2022)	α_H	0.52	Peter et al. (2022)
ψн	2.0	Peter et al. (2022)	δ_1	0.1	Usman and Adamu (2017)
ω_H	0.83	Giulio and Eckburg (2004)	δ_2	0.1	Usman and Adamu (2017)
β_H	0.93	Assumed	β_1	0.000063	Emeka et al. (2018)
θ_H	0.03	Assumed	eta_2	0.00025	Assumed <i>et al.</i> (2009)
β_3	0.01	Emeka et al. (2018)	μ_R	0.3	Emeka et al. (2018)
β_4	0.27	CDC (2018)	$ au_R$	0.3	Alakunle et al. (2020)
K	500	Madubueze et al., (2022)	${\cal E}_R$	0.4	Alakunle et al. (2020)
μ_B	0.003	Assumed	$ heta_R$	0.5	Assumed
ρ_1	0.04	Assumed	ψ_R	1.0	Peter et al. (2022)
ρ_2	0.02	Madubueze et al., (2022)		0.4	Assumed

Dynamic of sub-populations plotted against time

Emeka et al. (2018)

Dynamics of sub-populations plotted against time. The dynamics of sub-population plotted against time is presented in Figure 2. All the graphs were generated using values in Table 3 and Table 4 respectively.

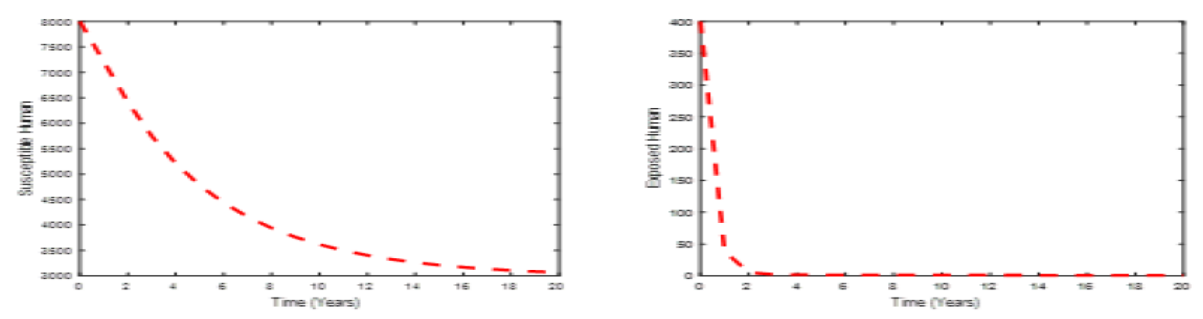


Figure 2: Dynamics of susceptible humans, and exposed humans plotted against time.

6.0.1 Dynamics of sub-populations plotted against time with varied human-human contact rate

The dynamics of sub-population plotted against time with varied β1 is presented in Figure 3. All the graphs were generated using values in table 3 and table 4 respectively.

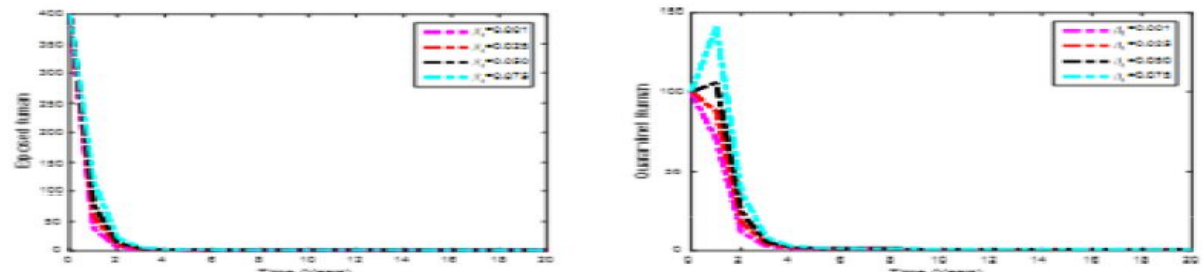
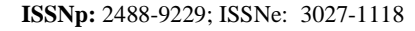


Figure 3: Dynamics of exposed human, and quarantined humans with varied β1 plotted against time.

6.0.2 Dynamics of sub-populations plotted against time with varied rodent-rodent contact rate

The dynamics of sub-population plotted against time with varied β4 is presented in Figure 4. All the graphs were generated using values in table 3 and table 4 respectively.



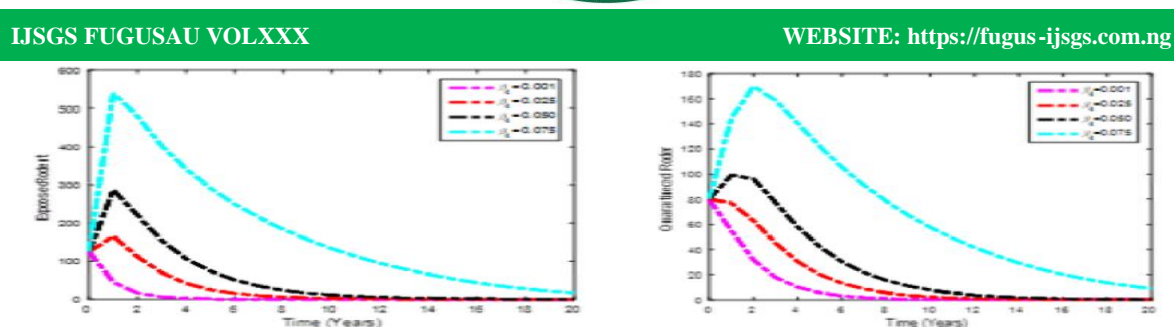


Figure 4: Dynamics of exposed rodent, and quarantined rodent with varied β4 plotted against time.

6.0.3 Dynamics of sub-populations plotted against time with varied environmental contact rate

The dynamics of sub-population plotted against time with varied $\beta 3$ is presented in Figure 5. All the graphs were generated using values in table 3 and table 4 respectively.

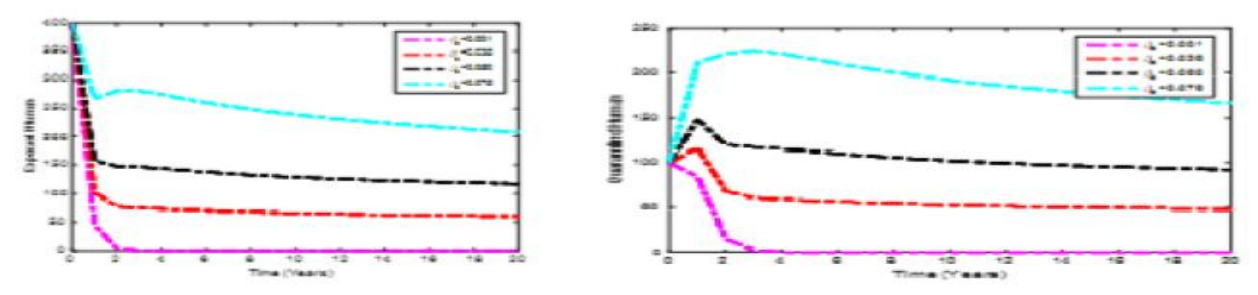


Figure 5: Dynamics of exposed humans, and quarantined human with varied β3 plotted against time.

7.0 RESULT DISCUSSION

In this section, analytical and numerical results were discussed.

7.1 Discussion of analytical results

There are twelve (12) differential equation systems in the monkey pox model. As a result, we demonstrated that the model's solution is positively invariant and attractive for the system for all time t. The positivity of the solutions to the system of differential equations must be non-negative. The free equilibrium states for monkey pox were discovered. The next generation matrix was also used to determine the basic reproduction number $\Box 0$. We used Castillo-Chavez, (2002) for global asymptotic stability of the monkey pox free equilibrium state. When $\Box 0 \Box \Box 1$, $\Box 0$ is locally asymptotically stable (LAS). Similar to this, the global stability of DFE was also calculated, and the results indicate that since the requirements for (GAS) are satisfied, the system is globally asymptotically stable. After the sensitivity index was calculated, the results indicated that parameters with positive indices increased the $\Box 0$, while those with negative indices decreased it. This suggests that the parameters have the power to either increase or decrease the prevalence of disease in the population.

7.2 Discussion of numerical results

In this section, the numerical discussions as presented in Figure 2 to Figure 5 are discussed as:

7.2.1 Dynamics of sub-populations plotted against time

In this section, we consider the sub-populations model of the system of differential equations in obtaining the dynamics of susceptible humans and exposed humans plotted against time via MATLAB R2016a. This describes the dynamical inter-play between human population leading to the model build - up. For the purpose of illustration, the initial values together with the parameter values in Table 3 and Table 4 are used to obtain the plots. The result shows a decrease in the behavior of the susceptible humans at different time interval. This is due to the infection, vaccination and natural death of susceptible humans. The result of exposed humans shows a rapid and steady decrease at different time interval. These depict movement to infected human compartment, quarantine human compartment and natural death

7.2.2 Dynamics of exposed human and quarantined human with varied human-human contact rate plotted against time

As illustrated in Figure 3, simulation of the model using a combination of human dynamics from exposed human and quarantined humans, with varied $\beta 1$, were ran as seen in the illustrations, if the transmission rate $\beta 1$ is initially high and then gradually declines, the number of exposed people will rise rapidly at first but then level off as the transmission rate decrease. In the initial stages, the



number of quarantined people might rise progressively, but as the transmission rate falls, the number of quarantined individuals might increase faster as the transmission falls rapidly.

7.2.3 Dynamics of exposed rodent and quarantined rodent with varied rodent-rodent contact rate plotted against time

In this simulation, the dynamics of a monkey pox virus induced by rodent, using a range of $\beta 4$ plotted against time as shown in Figure 4, were examined. It was observed that, the virus will spread slowly if $\beta 4$ is low. Over time, both the number of exposed and quarantined rodent will begin to increase. The virus will continue to have a low overall prevalence. If $\beta 4$ is increased, the virus will spread quickly. The number of exposed rodent and quarantined rodent will all rise quickly over time. If $\beta 4$ is increased gradually, there may be a threshold effect where the virus initially spreads slowly until the transmission rate reaches a certain level, after which the spread of the virus begins to decline.

7.2.4 Dynamics of exposed human and quarantined human with varied environmental contact rate plotted against time

Here, we simulated the dynamics of exposed human and quarantine human with varied β3 plotted against time as shown in Figure 5, we examined the spread of the virus caused by environmental transmission. The progression rate β_3 represents environmental transmission rate. We find that the number of infections increases with the number of infected humans who shed the infection into the environment. We found that when β_3 rises, so does the population's total number of infected persons. Furthermore, as β_3 declines, fewer people become infected in the population, which ultimately leads to the eradication of MPXV infection. Furthermore, as β_3 rises, so does the rate of quarantine. This indicates that, while quarantine measures by themselves are unable to stop the spread of MPXV in the community, they can be used in conjunction with other interventions to eradicate MPXV entirely. It was noted that if β_3 is low, the virus will propagate slowly over time.

resulting in a decline in the number of exposed and infected rodents as well as those kept in quarantine.

8.0 CONCLUSION

This study looked at the dynamics of monkeypox virus transmission and its analysis, using a modified version of the Madubueze *et al.*, (2022) work. The results shown that the solution to the model is positively invariant and attractive for the system for all time t. The positivity and boundedness of the solutions to the system of differential

WEBSITE: https://fugus-ijsgs.com.ng

equations were found. The free equilibrium states for monkey pox were discovered. The next generation matrix was also used to determine the basic reproduction number, R_0 . We used Castillo-Chavez, (2002), criteria approach to look into the system's global asymptotic stability of the monkey pox free equilibrium state. The result indicates that it is locally asymptotically stable (LAS) if R0 < 0. Likewise, the computation of DFE's global stability indicates that the system is globally asymptotically stable due to the satisfaction of the (GAS) criteria. After the sensitivity index was calculated, the results indicated that parameters with positive indices increased the R_0 , while those with negative indices decreased it. This suggests that the parameters have the power to either increase or decrease the prevalence of disease in the population. In order to evaluate the dynamics of monkey pox on the human population, a numerical simulation of the model was conducted using MATLAB R2016a. The findings were also addressed.

ACKNOWLEDGEMENT

The authors are thankful to the Department of Mathematics, Modibbo Adama University, Yola, Nigeria, where this research was initiated and carried out.

REFERENCES

Alakunle, E., Moens, U., Nchinda, G., & Okeke, M. I. (2020). Monkeypox virus in Nigeria: infection biology, epidemiology, and evolution. Viruses, 12(11), 1257.

Arotolu, T. E., Afe, A. E., Wang, H., Lv, J., Shi, K., Huang, L., & Wang, X. (2022). Spatial modeling and ecological suitability of monkeypox disease in Southern Nigeria. Plos one, 17(9), e0274325.

Awoyomi, O. J., Njoga, E. O., Jaja, I. F., Oyeleye, F. A., Awoyomi, P. O., Ibrahim, M. A., .& Oguttu, J. W. (2023). Mpox in Nigeria: Perceptions and knowledge of the disease among critical stakeholders—Global public health consequences. PloS one, 18(3), e0283571.

Brown, K., & Leggat, P. A. (2016). Human monkeypox: current state of knowledge and implications for the future. Tropical medicine and infectious disease, 1(1),

Chadha, J., Khullar, L., Gulati, P., Chhibber, S., & Harjai, K. (2022). Insights into the monkeypox : Making of another pandemic within the pandemic?. Environmental Microbiology, 24(10), 4547-4560.

Diekmann, O., Heesterbeek, J. A. P., & Roberts, M. G. (2010). The construction of next-generation matrices for compartmental epidemic models. Journal of the royal society interface, 7(47), 873-885.



WEBSITE: https://fugus-ijsgs.com.ng

IJSGS FUGUSAU VOLXXX

- Emeka, P. C., Ounorah, M. O., Eguda, F. Y., & Babangida, B. G. (2018). Mathematical model for monkeypox virus transmission dynamics.
 Epidemiology, 8, 348.
- Farahat, R. A., Sah, R., El-Sakka, A. A., Benmelouka, A. Y., Kundu, M., Labieb, F. & Rodriguez-Morales, A. J. (2022). Human monkeypox disease (MPX). Le infezioni in Medicina, 30(3), 372.
- Farasani, A. (2022). Monkeypox virus: Future role in Human population. Journal of Infection and Public Health.
- Jeyaraman, M., Selvaraj, P., Halesh, M. B., Jeyaraman, N., Nallakumarasamy, A., Gupta, M. & Gupta, A. (2022). Monkeypox: an emerging global public health emergency. Life, 12(10), 1590.
- Kannan, S., Ali, P., & Sheeza, A. (2022). Monkeypox: epidemiology, mode of transmission, clinical features, genetic clades and molecular properties. European Review for Medical & Pharmacological Sciences, 26(16).
- Lenglart, L., Ouldali, N., Honeyford, K., Bognar, Z., Bressan, S., Buonsenso, D.,& EPISODES Study Group. (2023). Respective roles of non-pharmaceutical interventions in bronchiolitis outbreaks: an interrupted time-series analysis based on a multinational surveillance system. European Respiratory Journal, 61(2).
- Madubueze, C. E., Onwubuya, I. O., Nkem, G. N., & Chazuka, Z. (2022). The transmission dynamics of the monkeypox virus in the presence of environmental transmission. Frontiers in Applied Mathematics and Statistics, 8, 1061546.
- Peter, O. J., Kumar, S., Kumari, N., Oguntolu, F. A., Oshinubi, K., & Musa, R. (2022) Transmission dynamics of Monkeypox virus: a mathematical modelling approach. Modeling Earth Systems and Environment, 1-12.
- Song, B., Castillo-Chavez, C., & Aparicio, J. P. (2002). Tuberculosis models with fast and slow dynamics: the role of close and casual contacts. Mathematical biosciences, 180(1-2), 187- 205.
- Usman, S., & Adamu, I. I. (2017). Modeling the transmission dynamics of the monkeypox virus infection with treatment and vaccination interventions. Journal of Applied Mathematics and Physics, 5(12), 2335.
- Van der Boom, M., & van Hunsel, F. (2023). Adverse reactions following MPox (monkeypox) vaccination: an overview from the Dutch and global adverse event reporting systems. British Journal of Clinical Pharmacology.